Computers and Electronics in Agriculture 212 (2023) 108165

Contents lists available at ScienceDirect

Computers and Electronics in Agriculture

journal homepage: www.elsevier.com/locate/compag

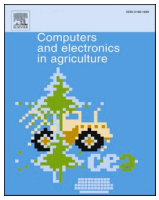

Influence of different soil reflectance schemes on the retrieval of vegetation LAI and FVC from PROSAIL in agriculture region

Haiying Jiang [a], Xiangqin Wei [b,*], Zhulin Chen [a], Mengxun Zhu [c], Yunjun Yao [a], Xiaotong Zhang [a], Kun Jia [a,*]

[a] State Key Laboratory of Remote Sensing Science, Faculty of Geographical Science, Beijing Normal University, Beijing 100875, China
[b] Aerospace Information Research Institute, Chinese Academy of Sciences, Beijing 100101, China
[c] Ecological Technology Research Institute, CIECC, Beijing 100048, China

ARTICLE INFO

Keywords:
Soil reflectance
PROSAIL model
Leaf index area (LAI)
Fractional vegetation cover (FVC)
GaoFen-1

ABSTRACT

The PROSAIL model is widely used to retrieve vegetation parameters from remote sensing data in agriculture regions. Soil reflectance is a key input to the PROSAIL model, but its influence on vegetation parameters retrieval accuracy of crops is rarely discussed. Therefore, this study investigated the influence of different soil reflectance schemes on leaf area index (LAI) and fractional vegetation cover (FVC) retrieval accuracy based on the PROSAIL model in an agriculture region. Firstly, three sources of soil reflectance including ICRAF-ISRIC soil spectral library (SR_SSL), general spectral vectors model (SR_GSV), and ASD spectroradiometer measurement (SR_ASD) and two reflectance extraction schemes were used to generate input soil reflectance for the PROSAIL model to simulate canopy reflectance. Then, the LAI and FVC retrieval models were developed using the random forest algorithm and validated using field survey data. Determination coefficient (R^2), Root Mean Square Error (RMSE) and normalized RMSE (NRMSE) were used to evaluate the accuracy of LAI and FVC retrieval. Under the direct extraction scheme, the LAI retrieval based on SR_ASD ($R^2 = 0.78$, RMSE = 0.613, NRMSE = 0.269) achieved better performance than SR_GSV ($R^2 = 0.73$, RMSE = 0.671, NRMSE = 0.294) and SR_SSL ($R^2 = 0.71$, RMSE = 0.762, NRMSE = 0.334), whereas the performances of FVC retrieval were comparable for SR_ASD ($R^2 = 0.91$, RMSE = 0.084, NRMSE = 0.136), SR_GSV ($R^2 = 0.90$, RMSE = 0.086, NRMSE = 0.139) and SR_SSL ($R^2 = 0.89$, RMSE = 0.091, NRMSE = 0.147). The influence of soil reflectance on LAI retrieval is larger than that of FVC in this study. Furthermore, soil reflectance was more important for canopies characterized by low LAI and FVC. In addition, the combination of SR_SSL and multiplication coefficients scheme could be conveniently used for large areas vegetation parameters retrieval. While SR_GSV and SR_ASD with direct extraction scheme was suitable for small areas with field survey data and more homogeneous region.

1. Introduction

Leaf area index (LAI) and fractional vegetation cover (FVC) are two essential vegetation parameters for describing structural property and growth status of land surface vegetation, which are important indicators for net primary production, water and nutrient use, carbon storage estimation, ecosystem health evaluation and agricultural monitoring (Bréda 2008; Jiang and Fang, 2019; Xia et al., 2021; Wang et al., 2018; Younes et al., 2019; Xie et al., 2019; Marandi et al., 2022). Therefore, accurate estimation of LAI and FVC for large areas is of great importance for related research, such as crop yield estimation, earth system science and sustainable development. Remote sensing techniques are effective for estimating vegetation parameters over large areas. Numerous approaches have been developed to estimate LAI and FVC from remote sensing data, such as the widely used method of integrating the PROSAIL radiative transfer model and machine learning techniques, particularly for crop canopy parameter estimation (Baret et al., 2007; Baret et al., 2013; Jia et al., 2016; Tao et al., 2021; Liu et al., 2021; Verrelst et al., 2016).

The PROSAIL model is composed of the leaf optical properties model PROSPECT and canopy bidirectional reflectance model SAIL, in which the leaf reflectance, leaf transmittance (both provided by PROSPECT) and soil reflectance (provided by the user) are three wavelength-dependent input variables (Jacquemoud et al., 2009). Many studies

* Corresponding authors.
E-mail addresses: weixq@aircas.ac.cn (X. Wei), jiakun@bnu.edu.cn (K. Jia).

https://doi.org/10.1016/j.compag.2023.108165
Received 28 March 2023; Received in revised form 13 August 2023; Accepted 18 August 2023
Available online 24 August 2023
0168-1699/© 2023 Elsevier B.V. All rights reserved.

have shown that soil reflectance is a major source of uncertainty for vegetation biophysical parameters retrieval using radiative transfer model (Darvishzadeh et al., 2008a; Vamborg et al., 2011). The variation of soil background has influence on LAI estimation using vegetation indices method and FVC estimation using the dimidiate pixel model at lower canopy cover, and root mean square error caused by soil reflectance in FVC estimation can reach 0.08 (Fu et al., 2013; Ding et al., 2016).

Usually, the soil reflectance used in PROSAIL model to simulate top-of-canopy reflectance can be obtained by various methods, such as radiative transfer model, empirical method, existing soil spectral library and field measured soil reflectance (Price 1990; Hapke 1993; Weiss et al., 2000; Jiang and Fang, 2019; Ding et al., 2022). Soil radiative transfer models often require multiple complex physical parameters and are rarely used in practice. Empirical methods often use a single typical spectral shape and brightness coefficient to characterize the soil reflectance, which makes it difficult to characterize the reflectance of different soils. For instance, the dry soil and wet soil spectra used in the PROSAIL model are linearly mixed using brightness coefficients to represent different soil conditions (Jacquemoud et al., 2009). Consequently, some large area vegetation parameter retrieval studies have employed multiple typical soil spectra, such as the CYCLOPES global LAI, fAPAR and FVC products algorithm and MODIS LAI product algorithm adopt 5 soil spectral samples from France and 25 soil spectral samples from the United States, respectively (Zhang et al., 2021; Knyazikhin et al., 1998). The ICRAF-ISRIC soil spectral library includes 4438 soil samples from 58 countries in Africa, Asia, Europe, North America and South America (Zhang et al., 2020; Garrity and Bindraban, 2004), and thus has the potential to better represent heterogeneous soil conditions in radiative transfer models with the aim of improving the retrieval accuracy of vegetation parameters from remote sensing data on the global scale. Therefore, many studies explored different numbers of typical soil spectra from the ICRAF-ISRIC soil spectral library to build simulated datasets using the PROSAIL model (Jia et al., 2016; Wang et al., 2018). However, the soil reflectance screened from the spectral library does not effectively represent the soil spectrum of a specific local area, and there may be some uncertainty in the retrieval of vegetation parameters. Spectral vectors models can simulate hyperspectral soil reflectance for the specified study area based on multi-spectral remote sensing data and global soil spectral characteristics. The representative general spectral vectors (GSV) model is developed based on the global dry and wet soil reflectance database, which can effectively simulate the soil reflectance for various soil conditions (Jiang and Fang, 2019). The key issues of the GSV model are the selection of bare soil pixels and the need for multi-spectral data of sufficient spectral resolution allowing the accurate modelling of hyperspectral soil reflectance data. Field measurement of soil spectrum can ensure the accuracy of soil information, but it is time-consuming and laborious to collect soil spectrum in a large area.

In summary, all methods to obtain accurate, applicable and representative soil spectral information have advantages and disadvantages, and therefore can lead to the error of vegetation parameters retrieval using the PROSAIL model. However, few studies have assessed the influence of soil reflectance on vegetation parameters retrieval from remote sensing data. Therefore, this study aims to investigate the influence of different soil reflectance schemes on the retrieval accuracy of LAI and FVC based on the PROSAIL model in the agriculture region.

2. Materials and methods

2.1. Study area and field experiments

The study area is located in Hengshui (115°10′E ~ 116°34′E, 37°03′N ~ 38°23′N), Hebei Province of China (Fig. 1). The study area is an alluvial plain with an elevation range of 12 to 30 m above sea level. The dominant land cover types in the study area are cropland and residential areas. Cropland is mainly characterized by the rotation of winter wheat and corn cultivation. The soil type in the study area is dominated by tawny soils, with soil textures dominated by neutral or slightly alkaline viscous clay.

The field experiments were conducted from March 29 to August 26, 2017 during the major crop growing season. Detailed information of the five experiments were provided in Table 1. Winter wheat was grown in

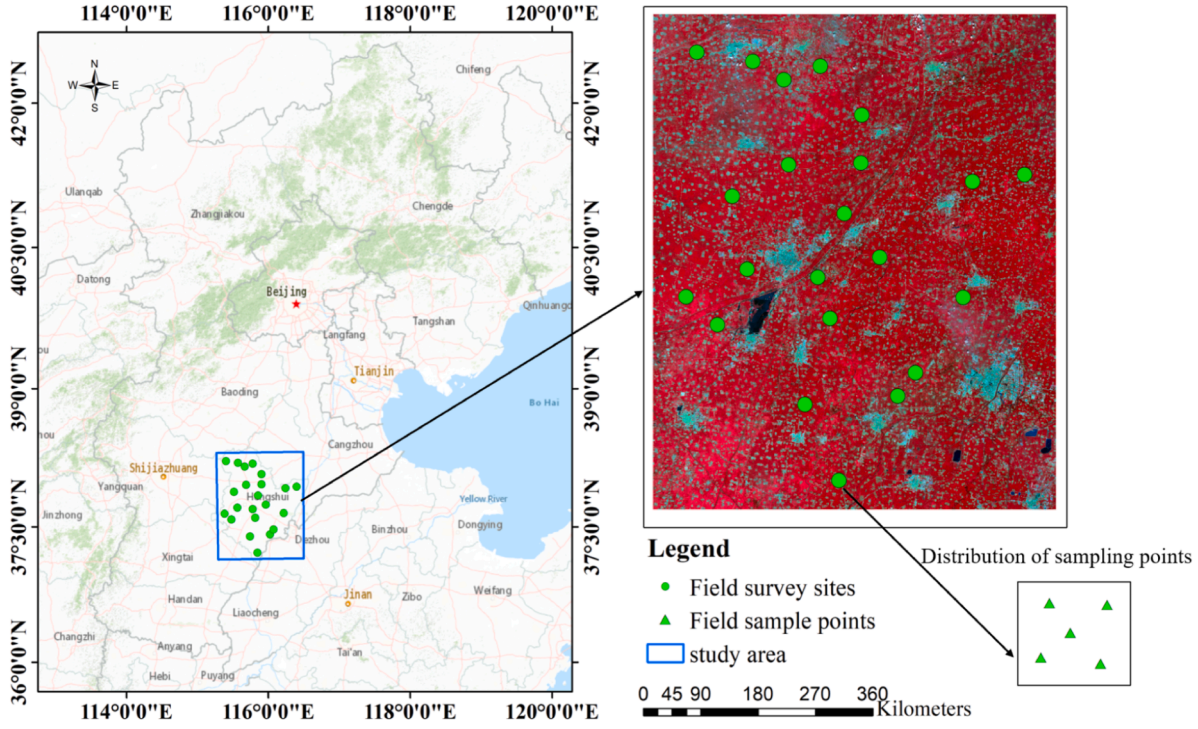

Fig. 1. The study area and field survey sites.

Table 1
The information of field experiments in Hengshui study area.

Experiment number	Start time	End time	Number of sites	Measured parameters	Crop type
1	2017–03-29	2017–04-01	21	LAI, FVC, soil spectra	Wheat
2	2017–05-04	2017–05-06	22	LAI, FVC, soil spectra	Wheat
3	2017–07-05	2017–07-08	23	LAI, FVC	Corn
4	2017–07-29	2017–08-01	22	LAI, FVC	Corn
5	2017–08-26	2017–08-29	22	LAI, FVC	Corn

the study area during the first and second experiments, which was from March 29 to May 6. For the next three experiments, which were conducted from July 5 to August 29, corn was grown in this period. During the five experimental investigations, the soil volume water contents were varied from 5.6% to 74.8%. Field crop parameters including LAI and FVC were collected. LAI was measured using the LAI-2200 canopy analyzer, while FVC was calculated using pictures taken perpendicular to the ground. Moreover, soil reflectance spectrum in the crop filed was measured using ASD spectrometer in the first and second experiments. Fig. 2 shows the typical soil spectra measured at one sampling site. About 20 sampling sites with dimensions of 100 m × 100 m were chosen for each field experiment. Each sampling sites was placed in the midst of a field of crops that had a generally homogeneous crop state. Each sampling site contains five small sampling points with a size of 30 m × 30 m. The LAI and FVC of each site were represented by the average values of the five sample points.

2.2. Data and data preprocessing

Four wide field view (WFV) cameras with 16 m spatial resolution are onboard the Chinese GaoFen-1 (GF-1) satellite, which have a combined swath of 830 km. The spectral parameters of GF-1 WFV sensors are given in Table 2. Fig. 3 shows the spectral response functions of the four WFV sensors in the four bands. The four sensors WFV1, WFV2, WFV3 and WFV4 of GF-1 have the same spectra band range but have slightly different spectral responses. In this study, six GF-1 WFV data (Table 3) covering the study area and the experimental period were obtained to retrieve vegetation parameters. The preprocessing of GF-1 WFV data included orthorectification and spatial registration to a global reference system (combined UTM projection and WGS84 ellipsoid), radiometric calibration and atmospheric correction. For the atmospheric correction, the FLAASH model was used as the port of the image processing software

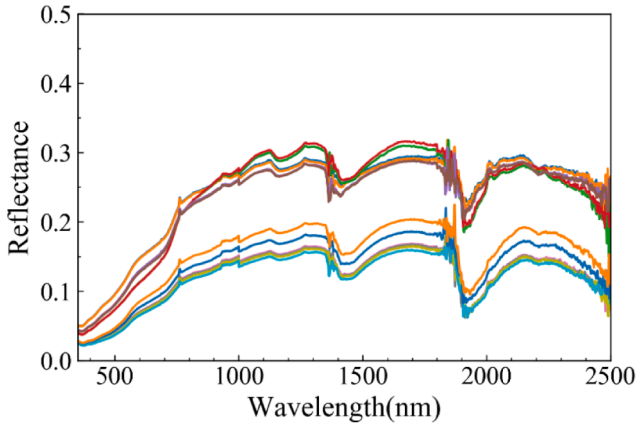

Fig. 2. The typical soil spectra measured by the ASD spectrometer at one sampling site.

Table 2
The spectral parameters of GF-1 WFV sensor.

Band name	Center wavelength	Wavelength range
Blue	485 nm	450 ~ 520 nm
Green	550 nm	520 ~ 590 nm
Red	660 nm	630 ~ 690 nm
Near infrared (NIR)	830 nm	770 ~ 890 nm

ENVI.

The Sentinel-2 satellite carries a multispectral imager (MSI), which provides 13 spectral bands with pixel sizes ranging from 10 to 60 m. Two Sentinel-2 images covering the study area on April 18 and April 28, 2017 were used to simulate the soil hyperspectral reflectance based on the GSV model. Atmospheric correction and resampling processing of Sentinel-2 image were performed using Sen2cor and SNAP software. Ten band reflectance including blue, green, red, red edge1, red edge2, red edge3, NIR, narrow NIR, SWIR1, and SWIR2 were used to simulate soil hyperspectral reflectance based on the GSV model.

The flowchart of this study is shown in Fig. 4. Firstly, three sources of soil reflectance were used as inputs to the PROSAIL model, in addition to two soil spectral extraction schemes were employed to select suitable representative soil spectral curves. Second, the PROSAIL model was used to the simulate canopy reflectance, and then the LAI and FVC estimation models were constructed using the random forest method based on the simulation datasets. Finally, the accuracy of the retrieved LAI and FVC was validated using the ground measured data.

2.3. Extraction of representative soil spectra

Three sources of soil reflectance were used in this study. The first soil reflectance source was the ICRAF-ISRIC soil spectral library (SR_SSL) with band range from 380 nm to 2500 nm and spectra interval of 10 nm. The second source was soil reflectance simulated by GSV model (SR_GSV) based on Sentinel-2 data. SR_GSV requires manually selecting soil pixels from the multi-spectral remote sensing data and then simulating corresponding hyperspectral soil reflectance using GSV model. Therefore, in order to eliminate the effects of vegetation, soil pixels should be selected from remote sensing data without vegetation coverage, preferably before crop planting or when bare soil pixels are present in the study area. When simulating the hyperspectral soil reflectance with GSV model, the accuracy of using the ten bands of Sentinel-2 was found to be much better than using the four bands of GF-1. Therefore, 409 soil pixels' multispectral reflectance extracted from the two Sentinel-2 images covering the study area are used to model the soil reflectance in this study. The third one was from 389 field measurements using ASD spectroradiometer (SR_ASD) in the study area from March 29 to April 1 and May 4 to 7, 2017, and soil spectral range was from 350 to 2500 nm with 1 nm interval. The SR_ASD contains the dry and wet soil reflectance in the study area. The raw ASD soil spectra were processed using a Gaussian smoothing method, as they fluctuated due to the impact of the monitoring devices and environmental factors.

To extract representative soil reflectance from the three sources of soil reflectance, the following processing was performed. First, the spectral functions of the GF-1 WFV sensor were used to calculate the reflectivity in the green, red, and NIR bands for each soil spectrum in the ICRAF-ISRIC, GSV model, and ASD measurements, respectively. Second, each 3-band soil spectrum was normalized by dividing the mean soil reflectance over the three bands, and then two extraction schemes were used to select representative soil reflectance.

For the first scheme (scheme 1), K-means method was conducted for the normalized spectral dataset to directly obtain 20 representative 3-band soil spectra. A widely used empirical method for modeling soil reflectance assumed that soil reflectance was proportional to a given spectral shape (Jiang and Fang, 2019), and multiple soil reflectance spectra could be obtained by multiplying the given typical soil spectra

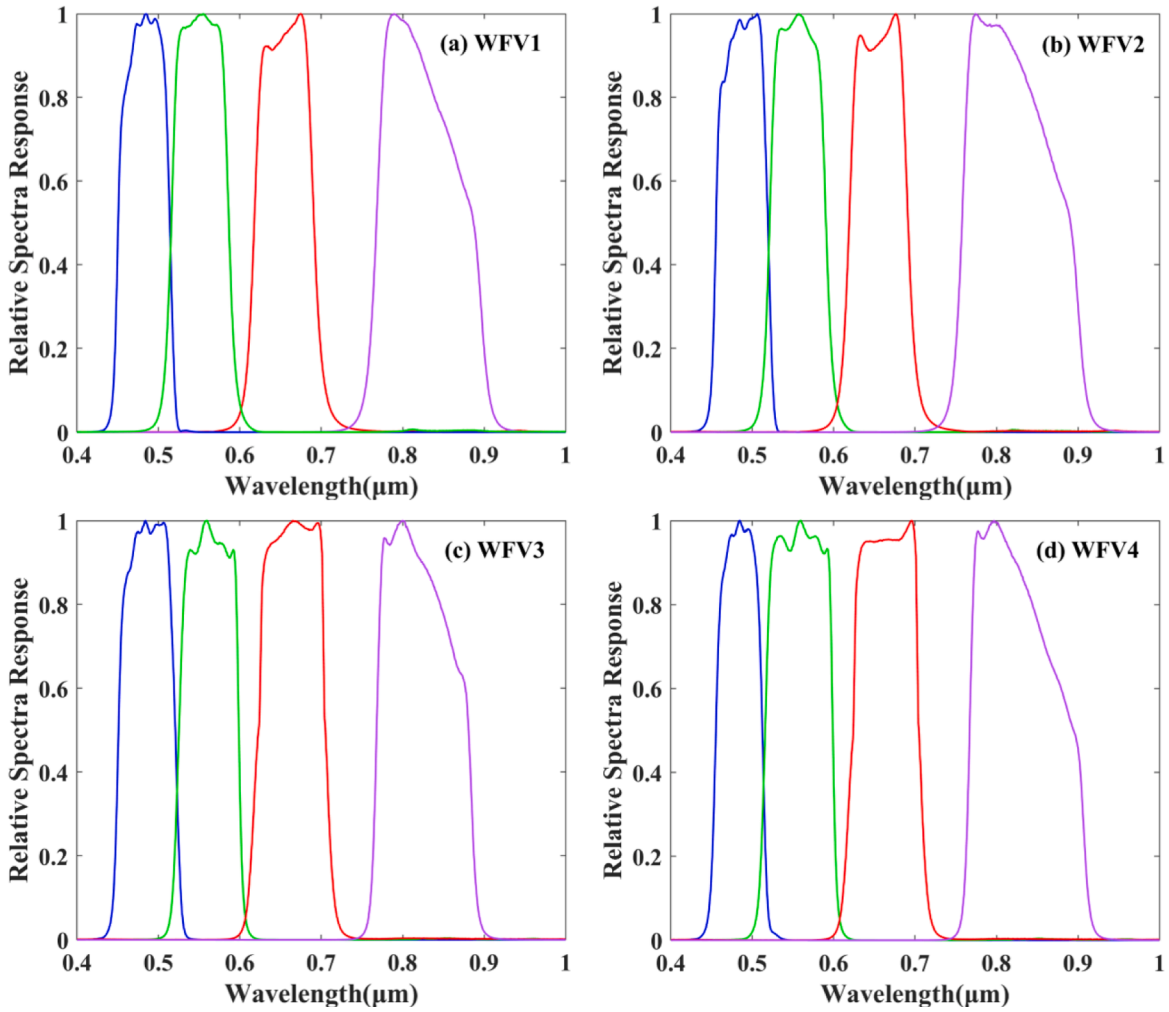

Fig. 3. The GF-1 WFV spectral response functions: WFV1 (a), WFV2 (b), WFV3 (c), WFV4 (d).

Table 3
The information of the acquired GF-1 WFV data.

Image date	Longitude and latitude of the scene center	Sensor
2017–04-01	E115.9°, N38.9°	WFV3
2017–04-01	E115.4°, N37.3°	WFV3
2017–05-07	E116.5°, N38.0°	WFV1
2017–07-08	E116.0°, N37.6°	WFV2
2017–08-10	E116.0°, N37.6°	WFV2
2017–08-30	E115.3°, N38.0°	WFV1

by the brightness coefficient (Baret et al., 2007; Qian and Liu, 2020). Therefore, the second scheme (scheme 2) of this study attempted to generate representative soil spectra based on brightness coefficient. For the scheme 2, the normalized spectral datasets were subjected to K-means to produce 5 groups of typical 3-band spectra, which were then multiplied by three brightness coefficients including 0.4, 1.2, and 1.6 to generate 20 representative soil reflectance data. The brightness coefficient could be considered as a way to adjust the overall brightness or intensity of the reflectance spectrum. By introducing the brightness coefficient, the magnitude of the input soil reflectance could be adjusted.

Based on scheme 1 and scheme 2, 20 representative soil reflectance with different overall magnitudes and different spectral shapes in green, red and NIR bands were generated from the three sources of soil reflectance, respectively. The spectral range was set to 400–1040 nm, which covers the spectral response functions of the GF-1 WFV sensors. It could be seen that the range of soil reflectance curves extracted from SR_SSL was larger than that from SR_GSV and SR_ASD, and the variation trend of SR_SSL was also different from SR_GSV and SR_ASD (Fig. 5). In addition, the soil reflectance curves extracted from SR_GSV and SR_ASD had similar trends.

2.4. Development of the LAI and FVC estimation models

The PROSAIL model (PROSAIL_D version) was used to generate the canopy reflectance simulation datasets with various vegetation parameters. The input parameters of PROSAIL model with a reasonable range to cover different land cover conditions were shown in Table 4. The input soil reflectance was extracted from SR_SSL, SR_GSV and SR_ASD using scheme 1 and scheme 2, respectively.

FVC was not an input parameter of the PROSAIL model, but the relationship between FVC and input parameters LAI and average leaf angle (ALA) could be established by the classical gap fraction. The relationship among FVC, LAI and ALA was expressed in the PROSAIL model with the following formulae (Nilson, 1971):

$$P_0(\theta) = e^{-\lambda_0 \frac{G(\theta,\theta_1)}{\cos\theta} \times LAI} \quad (1)$$

$$FVC = 1 - P_0(0) \quad (2)$$

where $P_0(\theta)$ was the gap fraction, θ was observation direction, $\theta 1$ was the ALA, G (θ, θ_1) was the orthogonal projection of a unit leaf area along direction θ. The parameter λ_0 was the leaf dispersion and was set to 1 (a

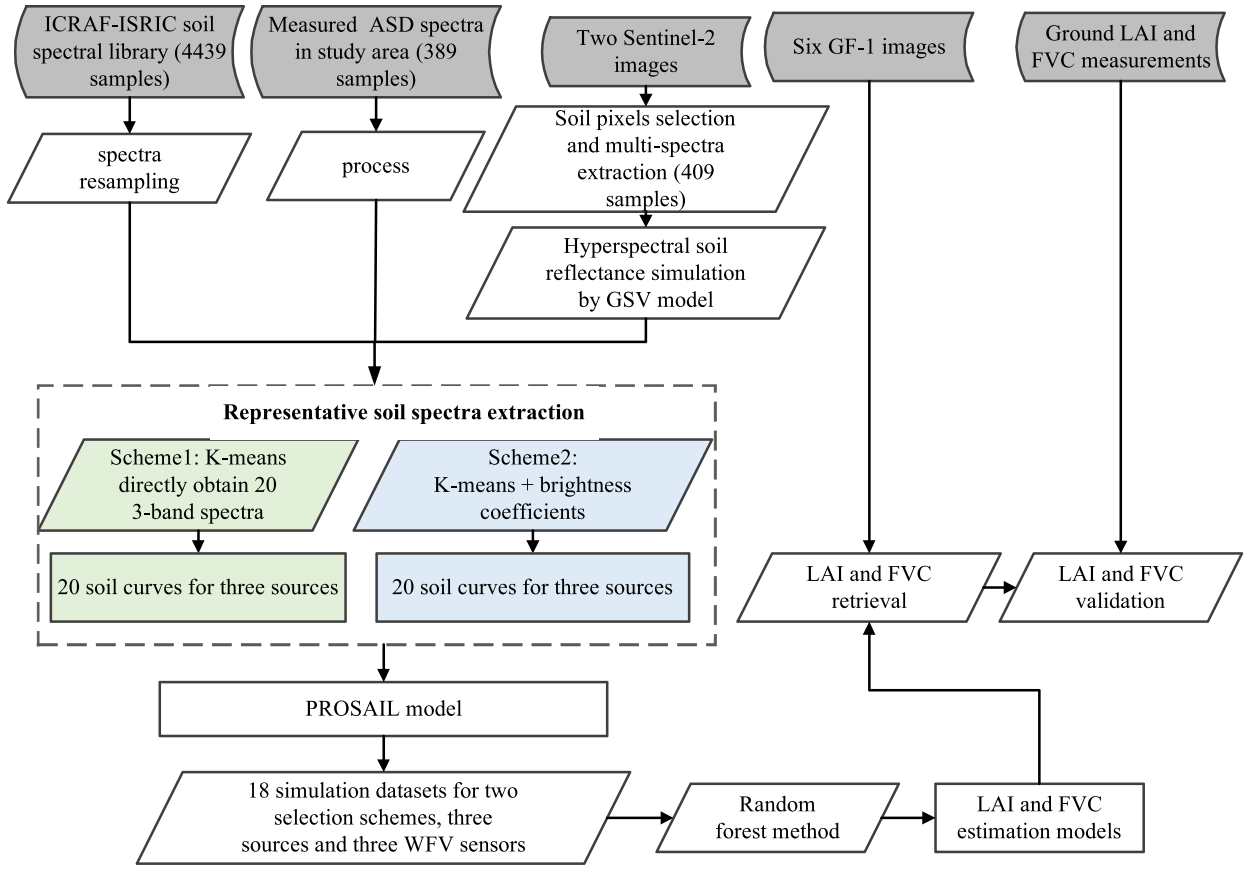

Fig. 4. The flowchart of this study.

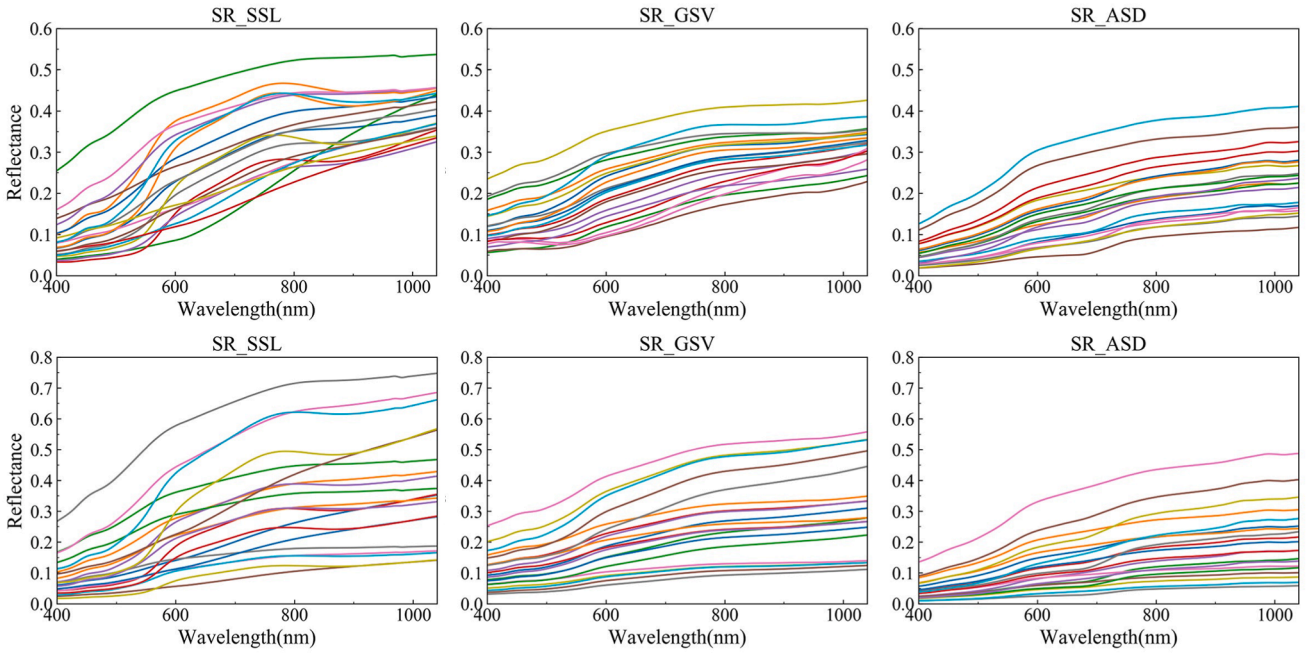

Fig. 5. Twenty representative soil reflectance curves for SR_SSL, SR_GSV and SR_ASD based on two extraction schemes for GF-1 WFV1 sensor (above is scheme 1, below is scheme 2).

random dispersion of foliage). According to the definition of FVC, FVC was calculated when θ was equal to 0 (Wang et al., 2018; Liu et al., 2021). According to formula (1) and (2), the association between FVC and PROSAIL model was established, and then the FVC could be calculated in the PROSAIL model simulation.

The canopy reflectance simulation using the PROSAIL model is as

Table 4
Parameter setting of the PROSAIL model.

Model	Variables	Variables definition	Unit	Range	Distribution	Mean	Std.
PROSPECT	C_{ab}	Chlorophyll a + b concentration	$\mu g/cm^2$	20–90	gaussian	45	30
	C_m	leaf dry matter content	g/cm^2	0.003–0.011	gaussian	0.005	0.005
	C_{ar}	leaf carotenoids content	$\mu g/cm^2$	4.4	–	–	–
	C_w	leaf water content	cm	0.005–0.015	uniform	–	–
	C_{brown}	Brown pigments content	–	0–2	gaussian	0.0	0.3
	C_{ant}	leaf anthocyanin content	$\mu g/cm^2$	0	–	–	–
	N	leaf structure parameter	–	1.25–2.2	uniform	1.5	0.3
SAIL	LAI	leaf area index	–	0–12	gaussian	2	2.0
	ALA	average leaf angle	deg	30–70	uniform	–	–
	Hot	hot spot parameter	–	0.1–0.5	gaussian	0.2	0.5
	SZA	sun zenith angle	deg	35	–	–	–
	VZA	view zenith angle	deg	0	–	–	–
	$RELAZ$	relative azimuth angle	deg	0	–	–	–

follows. First, reflectance and transmittance in the leaf layer are simulated the PROSPECT model. The parameters of PROSPECT model included leaf chlorophyll content (C_{ab}), carotenoid content (C_{ar}), leaf water content (C_w), leaf dry matter content (C_m), and leaf structure (N). Then, the SAIL model was used to simulate the interaction of light with the vegetation canopy. The SAIL model takes into account the optical properties of the leaves calculated by the PROSPECT model, as well as other canopy parameters such as LAI, ALA, and the soil reflectance. Next, the PROSAIL model is integrated with the results from the PROSPECT and SAIL models to produce the canopy reflectance from 400 to 1040 nm. Finally, the spectral response functions of GF-1 WFV were introduced to calculate the final band reflectance of GF-1 WFV1, WFV2, and WFV3.

Soil reflectance data from the three sources including ASD, GSV, and SSL, and two extraction schemes were used to generate the simulations for the three GF-1 WFV sensors. Furthermore, in order to accurately compare the performance of different soil reflectance and construct the PROSAIL training samples, the simulations had the same input parameter settings except for the soil reflectance for each training sample. The number for each variable in Table 4 was 10,000. Finally, 18 simulated datasets, each containing 200,000 items, were generated based on soil reflectance from the three sources and two extraction schemes and three WFV sensors. The 18 datasets had the same leaf parameters, canopy structure parameters and observed geometry parameters. Six different types of input soil reflectance could be produced by the three sources of soil reflectance and two extraction schemes for each WFV sensor.

Random forest regression (RFR) is a supervised learning algorithm that used ensemble learning method for regression (Doktor et al. 2014). In this study, the RFR method was used to construct the LAI and FVC estimation models with PROSAIL simulation datasets. Each simulation dataset was divided into two parts, with 80% of the data used for training data and the remaining 20% for validation. Green, red and NIR band reflectance were used as the input variables and LAI or FVC as output variables. In order to compare the LAI and FVC retrieval accuracy using SR_SSL, SR_GSV and SR_ASD, the LAI and FVC retrieval were validated based on the simulated data and field measured data with root mean square error (RMSE), normalized root mean square error (NRMSE) and coefficient of determination (R^2) as indicators. The calculation of RMSE and NRMSE is shown in formula (3) and formula (4). Except for the soil reflectance, the other parameter settings were fixed for generating samples of each model. Each simulation dataset used the same ordinal number to extract the training data. Therefore, the difference in accuracy of these models is mainly attributed to the difference in soil reflectance, although the RFR algorithm may have some minor effect.

$$RMSE = \sqrt{\frac{\sum_{i}^{N}(P_i - O_i)^2}{N}} \tag{3}$$

$$NRMSE = \frac{RMSE}{\overline{O}} \tag{4}$$

where P_i and O_i are the prediction and observation, respectively, N is the number of observations, and —O is the mean of the observations (Hupet et al., 2002; Dimitriadou and Nikolakopoulos, 2022).

3. Results

3.1. LAI and FVC estimation model validation based on the simulated data

Based on the simulated data, LAI and FVC estimation models were validated. Table 5 shows the R^2, RMSE, and NRMSE of LAI and FVC retrieval for different soil reflectance and extraction schemes based on the simulated dataset of WFV1 sensor. Overall, the differences between the LAI and FVC estimation models under the two extraction schemes were not significant. The estimation accuracy of LAI and FVC under scheme 1 is slightly worse than that under scheme 2. For LAI, the differences of NRMSE and RMSE of the two schemes under SR_ASD soil source were 0.021 and 0.057, respectively, which were larger than another two soil reflectance sources. For FVC, there was a slight difference between the two schemes with NRMSE less than 0.006 under the same soil reflectance source. The different performance of the two schemes could be explained by the different distributions and intensities of the selected soil spectra. By comparing the NRMSE values of the LAI and FVC estimation models, it can be found that the error of the LAI estimation model is obviously larger than that of the FVC estimation model. In addition, from the differences in the NRMSE values of LAI and FVC estimates for different sources of soil reflectance, the input different soil reflectance does not significantly affect on the estimation model accuracy.

Based on the soil reflectance extracted by scheme 1, the accuracy of LAI and FVC estimation model under different sensors and different sources of soil reflectance was discussed. The LAI validation results based on the simulated data were shown in Fig. 6. It could be seen that the accuracies of LAI estimation for the WFV1, WFV2, and WFV3 sensors were very similar when using the same input soil reflectance. This is because the three GF-1 WFV sensors have similar configurations with only minor differences in the spectral response function. Furthermore, the LAI validation accuracies for the same sensor with different sources of input soil reflectance were slightly different, but not significantly. The maximum differences of RMSE and R^2 were 0.074 and 0.035, respectively. In addition, it could be seen that the LAI estimation uncertainty becomes higher as the LAI value increases, which could be caused by the saturation of red reflectance at moderate-to-high vegetation density. Fig. 7 showed the FVC validation results using the simulated data, which indicated the satisfactory performances with $R^2 \geq 0.963$ and RMSE $\leq$ 0.05 for all different kinds of soil reflectance and different GF-1 sensors. For different sensors, similar to Fig. 6, the FVC validation accuracies

Table 5
R^2, RMSE and NRMSE of LAI and FVC retrieval for different soil reflectance and extraction schemes (based on WFV1 sensor simulated dataset).

Parameters	Soil sources	Scheme 1			Scheme 2		
		R^2	RMSE	NRMSE	R^2	RMSE	NRMSE
LAI	SR_SSL	0.781	0.885	0.304	0.825	0.920	0.316
	SR_GSV	0.779	0.896	0.308	0.825	0.914	0.314
	SR_ASD	0.747	0.949	0.325	0.790	1.006	0.346
FVC	SR_SSL	0.966	0.047	0.067	0.971	0.044	0.063
	SR_GSV	0.969	0.046	0.066	0.973	0.042	0.060
	SR_ASD	0.965	0.048	0.069	0.968	0.046	0.066

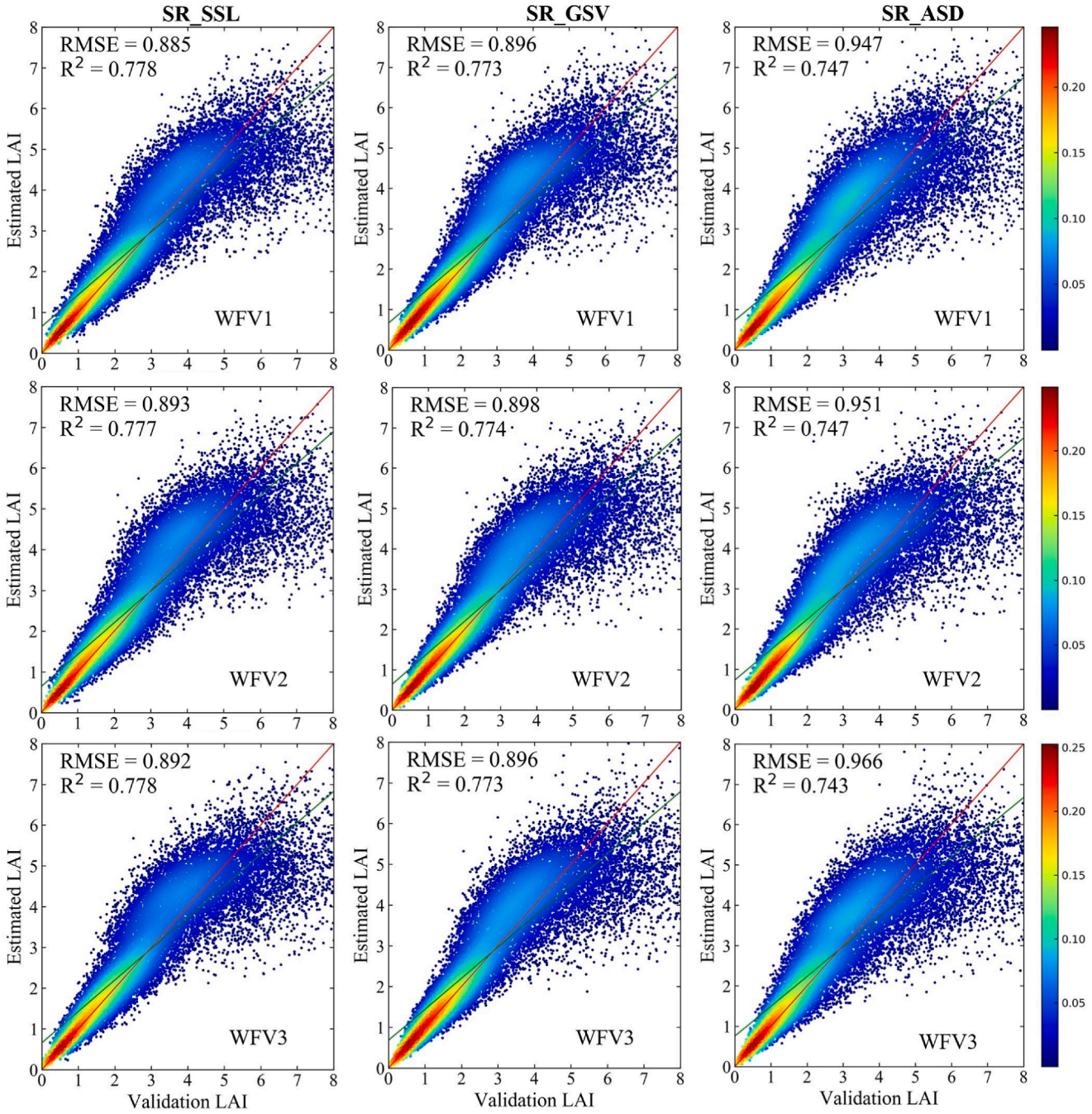

Fig. 6. LAI estimates validation based on the simulated data (under scheme 1).

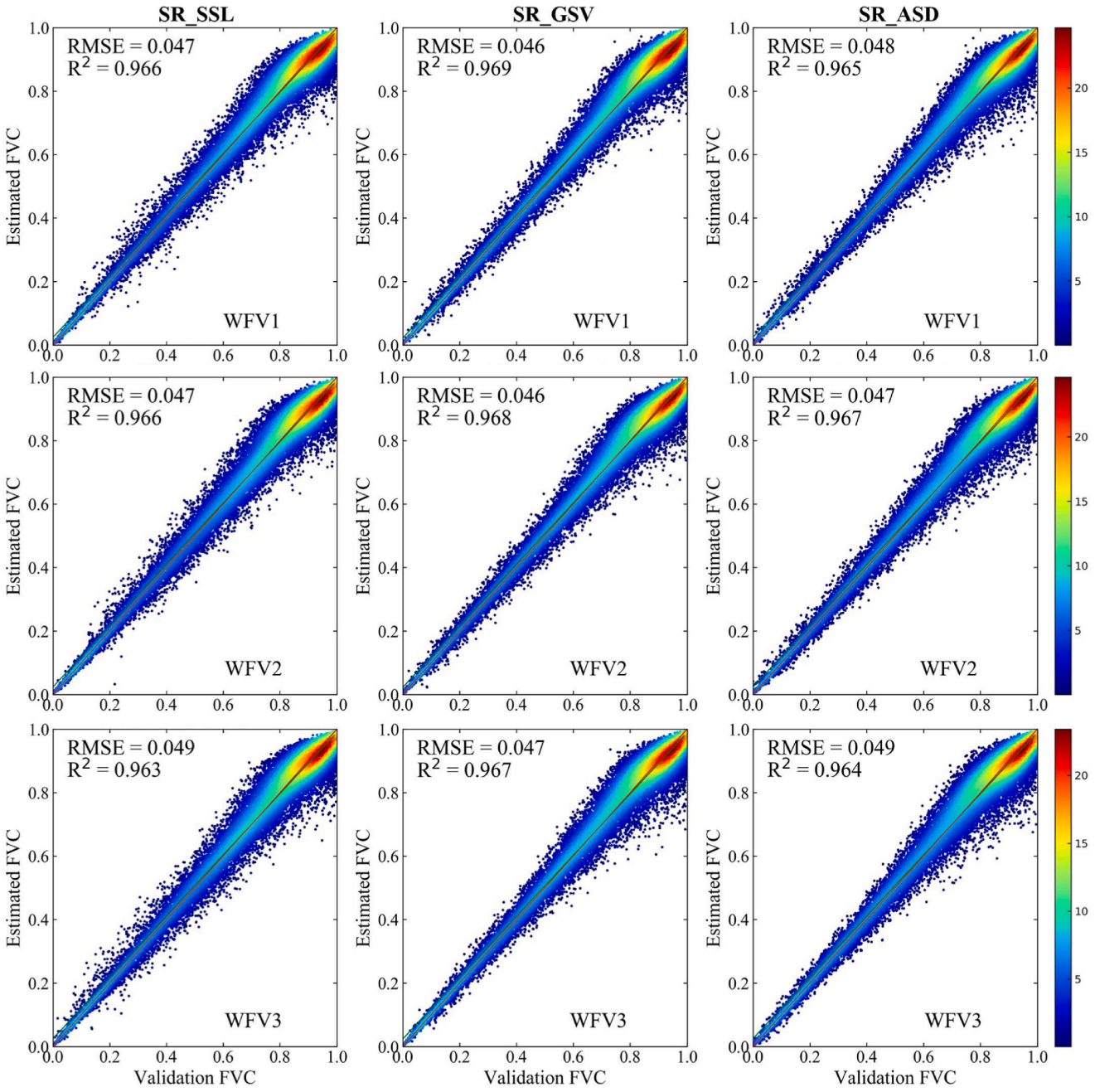

Fig. 7. FVC estimates validation based on the simulated data (under scheme 1).

were very close with the same kind of input soil reflectance. For different input soil reflectance, it could be found that the difference in FVC validation accuracy was almost negligible with the maximum RMSE of 0.004. By comparing LAI and FVC estimation models, it could be observed that the accuracy of FVC estimation model was much higher than that of LAI.

Table 6
R^2, RMSE and RMSE of LAI and FVC retrieval for different soil reflectance and extraction schemes (based on WFV1 sensor).

Parameters	Soil sources	Scheme 1			Scheme 2		
		R^2	RMSE	NRMSE	R^2	RMSE	NRMSE
LAI	SR_SSL	0.71	0.762	0.334	0.72	0.764	0.335
	SR_GSV	0.73	0.671	0.294	0.72	0.732	0.321
	SR_ASD	0.78	0.613	0.269	0.75	0.699	0.307
FVC	SR_SSL	0.89	0.091	0.147	0.89	0.090	0.146
	SR_GSV	0.90	0.086	0.139	0.89	0.090	0.146
	SR_ASD	0.91	0.084	0.136	0.90	0.086	0.137

3.2. Validations based on the ground measured data

Based on the remote sensing data reflectance, the LAI and FVC were retrieved by the LAI and FVC estimation models, respectively. Table 6 shows the R^2, RMSE, and NRMSE of LAI and FVC retrieval under different soil reflectance and extraction schemes based on the ground measured data. The soil reflectance extracted from SR_ASD by scheme 1 achieved the best performance for LAI and FVC estimates. It was notable that the LAI and FVC accuracies were significantly better under scheme 1, when the soil reflectance source was SR_GSV or SR_ASD, as compared to scheme 2. Compared with scheme 2, scheme 1 could reduce the RMSE of LAI by 0.061 and 0.086, and the RMSE of FVC by 0.004 and 0.002, using SR_GSV and SR_ASD, respectively. However, for SR_SLL, both scheme 1 and scheme 2 exhibit comparable LAI and FVC retrieval accuracies. This could be explained that when the study area was small, the representative soil reflectance curves (scheme 1) extracted directly from a certain number of measured or simulated soil reflectance were closer to the real situation. While in scheme 2, the extracted soil reflectance needs to be multiplied by the coefficients, whose values would affect the accuracy of LAI and FVC retrieval. Under the same extraction scheme, SR_ASD performs best and SR_SLL performs worst among the three sources of soil reflectance. Under scheme 1, the retrieval accuracy of LAI and FVC based on the soil reflectance from different sources is more different. In either case, the NRMSE of LAI is higher than that of FVC, which is consistent with the simulation data validation results. Additionally, the difference in NRMSE of LAI is greater than that of FVC under varied soil reflectance. The maximum NRMSE difference of the LAI under scheme 1 for various sources of soil reflectance was 0.065, whereas the maximum NRMSE difference of the FVC under scheme 1 for various sources of soil reflectance was 0.011. This indicates that LAI is more sensitive to soil reflectance than FVC.

Based on scheme 1, the performances of the three soil reflectance sources were discussed (Fig. 8). The PROSAIL with SR_ASD as input soil reflectance had achieved the best LAI and FVC retrieval accuracies, followed by SR_GSV, and SR_SSL performed worst. Compared to SR_SSL, using SR_ASD and SR_GSV could significantly improve the accuracy of LAI retrieval, with a RMSE reduction of 0.149 and 0.091, respectively. For FVC, using SR_ASD and SR_GSV reduces the RMSE by 0.005 and 0.007, respectively, with little improvement in the accuracy. Therefore, the three different sources of soil reflectance had less effect on the FVC retrieval accuracy than on the LAI. To adequately assess the performance, the NRMSE and mean absolute error (MAE) for different ranges of LAI and FVC were calculated based on the ground measured data (Table 7). Regardless of the soil reflectance source, the NRMSE of LAI and FVC with low values were significantly larger than that of LAI/FVC with high values. In the low and high LAI categories, the maximum NRMSEs difference between the three soil reflectance sources were

Table 7
NRMSE and MAE of LAI and FVC retrieval at different LAI and FVC ranges (based on scheme 1).

LAI and FVC Categories	Soil reflectance sources	NRMSE	MAE
Low LAI (0–3)	SR_SSL	0.436	0.549
	SR_GSV	0.332	0.467
	SR_ASD	0.354	0.489
High LAI (>3)	SR_SSL	0.283	0.858
	SR_GSV	0.254	0.832
	SR_ASD	0.237	0.817
Low FVC (0–0.4)	SR_SSL	0.265	0.050
	SR_GSV	0.231	0.047
	SR_ASD	0.254	0.043
Medium FVC (0.4–0.8)	SR_SSL	0.172	0.086
	SR_GSV	0.159	0.081
	SR_ASD	0.168	0.085
High FVC (0.8–1)	SR_SSL	0.107	0.070
	SR_GSV	0.105	0.066
	SR_ASD	0.097	0.065

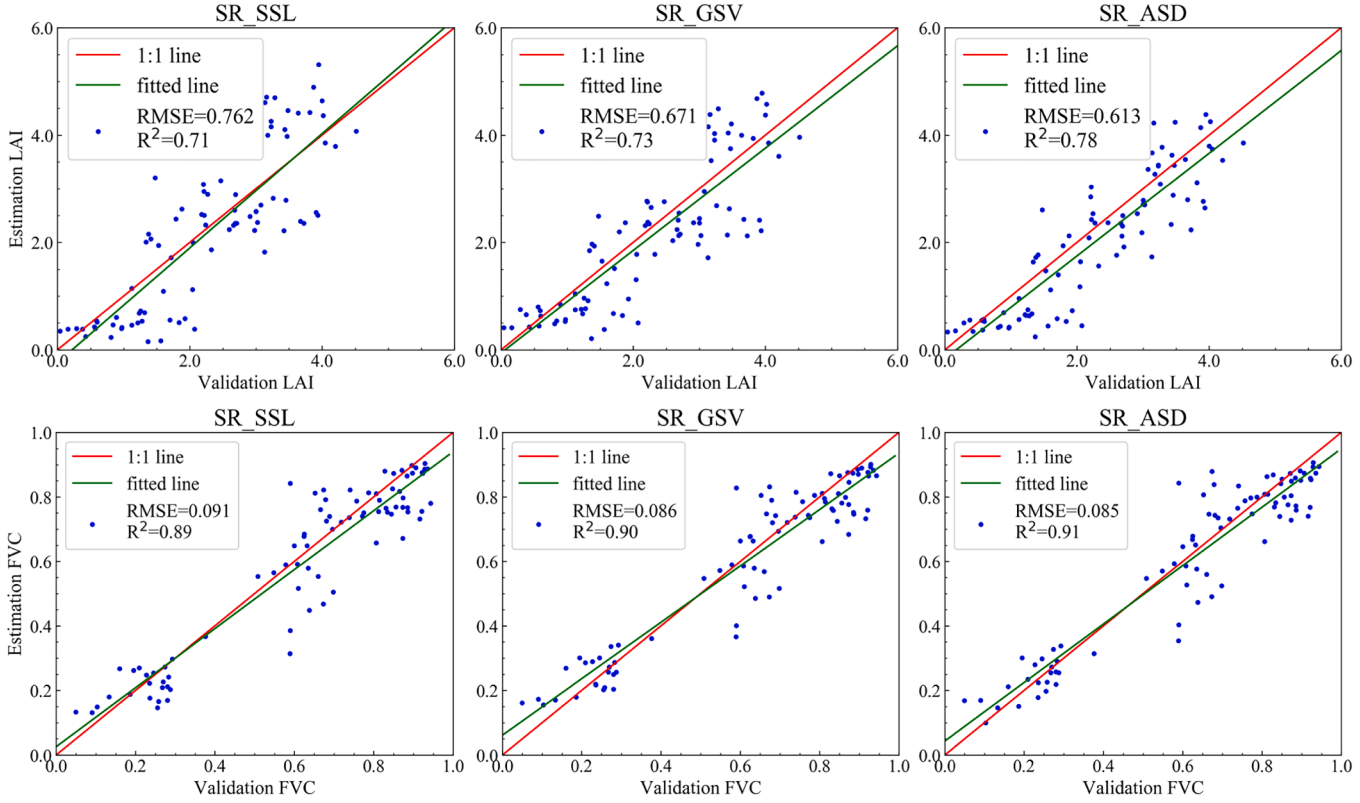

Fig. 8. LAI and FVC validation based on the ground measured data (under scheme 1).

0.104 and 0.046, respectively. As for the three FVC categories (low, medium, and high), the maximum differences in NRMSEs among the three categories were 0.034, 0.013, and 0.01, respectively. Furthermore, the MAEs of the three soil reflectance sources also showed greater differences in the low LAI/FVC categories. In the low and high LAI categories, the maximum MAEs difference between the three soil reflectance sources were 0.082 and 0.041, respectively. As for the three FVC categories, the maximum differences in MAEs among the three categories were 0.007, 0.005, and 0.005, respectively. Therefore, it could be indicated that the difference in LAI/FVC retrieval accuracy caused by different soil reflectance decreased with the increase of vegetation coverage.

4. Discussion

4.1. Soil reflectance influence on the LAI and FVC estimation

The validation results based on the simulated data show that the accuracies of LAI and FVC estimation models are different for different soil reflectance inputs. This is because the vegetation-to-soil reflectance ratio changes when the soil reflectance varies. This leads to a change in the vegetation reflectance value at different soil reflectance, which affects the output of the LAI and FVC estimation models. In addition, differing spectral response functions with the same PROSAIL model parameter settings result in varying reflectance of computed band reflectance, which also causes variations between the LAI and FVC estimation models. The results are consistent with the previous studies, such as Ding et al. (2017) find the FVC estimation models based on different vegetation indices have different sensitivity to soil background. The sensitivity of some FVC estimation models increases with soil reflectance, while the sensitivity of other FVC estimation models decreases with soil reflectance. A recent research by Gao et al. (2022) suggests the significant impact of background reflectance variability on the spectral response of agronomic variables, which can result in inconsistencies of the vegetation-LAI relationship. The simulation data validation results show that the estimation models corresponding to SR_SSL and SR_GSV had better FVC estimation accuracy under scheme 2, while the estimation accuracy under SR_ASD is the worst. However, with ground measured data validation, SR_ASD achieves the best validation results under scheme 1. This is because the estimation performance based on ground measured data is affected by both the parameter setting of the PROSAIL model and the accuracy of the estimated model. If the estimation model is not well suited to the characteristics of the measured data, even if it performs well on simulated data, it may still achieve poor performance with the measured data. In summary, the accuracy of vegetation parameters retrieval in practical applications is related to the parameters setting of PROSAIL model and the sensitivity of the vegetation parameters to the band reflectance. The soil reflectance can significantly impact the simulation of canopy reflectance, leading to potential inaccuracies in the retrieval of vegetation parameters.

The validation results based on ground data show that soil reflectance has a greater impact on LAI and FVC retrieval accuracy when vegetation coverage is low. When the vegetation density is high, the influence of soil reflectance on LAI retrieval is obviously reduced. This conclusion aligns with previous research that soil background influences on canopy reflectance would approach a maximum level at low vegetation densities, and when canopy coverage is close to 75%, soil background still has a certain influence on the greenness measures (Huete et al., 1985). According to research conducted by Prudnikova et al. (2019), the regions of 350–500 nm and 620–690 nm exhibit the most notable soil background effect, and the impact of soil reflectance on canopy reflectance varies with the developmental stages of wheat. The influence of soil reflectance on the reflectance of different bands of canopy is different, which leads to the different degree of influence of soil reflectance on the retrieval of different vegetation parameters. The research also highlights that LAI retrieval exhibits higher sensitivity towards soil reflectance than FVC retrieval, as shown by the validation based both on the simulated data and ground data. Red band reflectance decreases with increasing LAI, whereas near-infrared band reflectance increases (Huete, 1989). When LAI $>$ 4, the reflectance of red band reaches saturation and no longer decreases with the increase of LAI (Darvishzadeh et al., 2008b). As the vegetation density increases, the LAI increases correspondingly, whereas the FVC initially increases before plateauing at its maximum value of 1. Therefore, it can be inferred that the overall accuracy of LAI retrieval will decrease more due to the influence of soil reflectance. Observable from Fig. 6 and Fig. 7 is the comparatively lower accuracy of the LAI estimation model compared to that of the FVC, thus resulting in an increased sensitivity of the LAI to changes in reflectance. It can be indicated that soil reflectance exerts more influence on LAI retrieval.

4.2. Applicability of different soil reflectance sources and extraction schemes

The suitability and extraction schemes of the three soil reflectance sources need to be considered in combination. The SR_SSL source comprises soil reflectance data of varied soil types and conditions globally, rendering it ideal for vegetation parameter retrieval on a large scale. Directly extracting soil reflectance from SSL to input PROSAIL model may lead to obvious vegetation parameter retrieval errors. When SR_SSL is chosen as the input soil reflectance, scheme 2 is more suitable to extract representative soil spectra. It is necessary to combine prior knowledge to select the typical soil spectra consistent with the study area. Then, more representative soil spectra can be obtained by multiplication with appropriate brightness coefficients, so as to improve the localization and achieve superior retrieval performance.

For the SR_GSV source, the simulation accuracy of hyperspectral soil reflectance will be more accurate as the number of multi-spectral bands increases. This reinforces the potential of SR_GSV to achieve optimal performance for vegetation parameter estimation within a specific area, primarily in the presence of the requisite number of multi-spectral bands in remote sensing data, as well as an adequate selection of soil pixels that cover the diverse soil conditions in the study area. When the reflectance of the selected image soil pixels is sufficiently representative, scheme 1 can select the effective input soil reflectance for the PROSAIL model. However, when there are few image soil pixels, the simulated soil spectra cannot represent the whole study area. Therefore, it is necessary to expand the simulated soil spectra through scheme 2.

SR_ASD is highly preferred for retrieval of vegetation parameters in very small areas, because it is the true soil reflectance measured in the study area. Nonetheless, conducting soil reflectance measurements in the study area necessitates extensive field experiments that involve a significant expenditure of time and labor. Consequently, SR_ASD is shown to be the more optimal choice for carrying out vegetation parameter retrieval in smaller experimental areas. Since SR_GSV and SR_ASD are close to the true soil reflectance, a better parameter retrieval accuracy can be achieved by directly selecting the representative soil reflectance. For these two sources of soil reflectance, generating representative soil spectra by multiplying brightness coefficients may reduce the accuracy of soil reflectance. However, in cases where the measured soil spectral data is insufficient to reflect the soil reflectance of the study area, it becomes imperative to acquire more soil spectra through brightness coefficients.

4.3. Potential and limitations

Monitoring crop growth, predicting yield, and managing production all benefit from the retrieval of crop indicators with remote sensing data. Given that the PROSAIL model is frequently used for crop parameter retrieval and soil reflectance is one of its primary inputs, its impact on parameter retrieval accuracy cannot be ignored. This study demonstrates that under various soil reflectance sources and representative soil

reflectance extraction schemes, the retrieval accuracy of vegetation parameters varies. The sensitivity of various crop parameters to soil reflectance is different. LAI is substantially more impacted by soil reflectance than FVC. For crop parameter retrieval to be more precise, the proper soil reflectance input is crucial. Especially for parameters such as LAI that are sensitive to soil reflectance, when vegetation density is low, the retrieval accuracy is greatly affected by soil reflectance. This study further analyzes the applicability of different soil reflectance sources and extraction schemes and offers recommendations for input soil reflectance at various regional scales.

The influence of soil reflectance on canopy reflectance varies with soil type, soil moisture, soil organic matter content and soil roughness (Huete et al., 1985; Prudnikova et al., 2019). In this study, the differences of soil with different properties were qualitatively considered when collecting soil spectra. The soil type in this study area is single, and soil brightness, soil humidity and soil of different growth periods were considered during the experimental measurement. In addition, hundreds of pixels containing different soil brightness or moisture were selected in the screening of soil pixels. The ICRAF-ISRIC soil spectrum library contains soil spectra of different soil types, textures, moisture, and roughness. In order to extract the representative soil spectra, K-means method was used to extract the soil spectra with large differences. This study only considers the soil reflectance of different properties qualitatively, and further research can quantitatively analyze the influence of soil properties on the retrieval of vegetation parameters. The soil type in this study area is single, so the further research can validate the vegetation parameter retrieval accuracy under different soil types. In addition, the influence of soil reflectance on the canopy reflectance of various crops may different due to the varying structural features and planting structures. Only two crops are taken into account in this study, and additional research can examine how other crops' parameter inversions affect soil reflectance.

5. Conclusions

The influence of different soil reflectance sources and extraction schemes on the retrieval of vegetation LAI and FVC from PROSAIL model was investigated in the agriculture region. It was found that the influence of soil reflectance on LAI retrieval was larger than that of FVC, and the SR_ASD achieved the best LAI retrieval accuracy, followed by SR_GSV and SR_SSL. Compared with the multiplication coefficient scheme, directly extracting representative soil reflectance from SR_GSV and SR_ASD could obtaining better LAI and FVC retrieval accuracies for small study areas. For SR_SSL, the LAI and FVC retrieval accuracy of direct extraction scheme and multiplication coefficient scheme had no significant difference. Comparing LAI/FVC performance in different ranges, it was indicated that soil reflectance was more important in low LAI/FVC cases. In addition, considering the applicability of the three soil reflectance sources, SR_SSL was more suitable for global or large area vegetation parameters estimation, SR_GSV was a good choice when the study area was small and homogeneous, and the bare soil pixels were easily selected from the multi-spectral remote sensing data, and SR_ASD was more preferred for very small area with homogeneous soil conditions.

CRediT authorship contribution statement

Haiying Jiang: Methodology, Writing – original draft. **Xiangqin Wei:** Data curation, Formal analysis, Conceptualization, Writing - review & editing. **Zhulin Chen:** Software. **Mengxun Zhu:** Investigation. **Yunjun Yao:** Software, Validation. **Xiaotong Zhang:** Writing - review & editing. **Kun Jia:** Conceptualization, Methodology, Supervision.

Declaration of Competing Interest

The authors declare that they have no known competing financial interests or personal relationships that could have appeared to influence the work reported in this paper.

Data availability

Data will be made available on request.

Acknowledgements

This work was funded by the National Natural Science Foundation of China (No. 42171318 and No. 42192581), the Second Tibetan Plateau Scientific Expedition and Research Program (2019QZKK0405), and the Tang Scholar Program (K. Jia is a Tang Scholar of Beijing Normal University).

The authors would like to thank Prof. Hongliang Fang from institute of Geographic Sciences and Natural Resources Research of Chinese Academy of Sciences for providing the algorithm of GSV model.

References

Baret, F., Hagolle, O., Geiger, B., Bicheron, P., Miras, B., Huc, M., Berthelot, B., Nino, F., Weiss, M., Samain, O., Roujean, J.L., Leroy, M., 2007. LAI, FAPAR and FCover CYCLOPES Global Products Derived from VEGETATION. Remote Sens. Environ. 110 (3), 275–286. https://doi.org/10.1016/j.rse.2007.02.018.

Baret, F., Weiss, M., Lacaze, R., Camacho, F., Makhmara, H., Pacholcyzk, P., Smets, B., 2013. GEOV1: LAI and FAPAR Essential Climate Variables and FCOVER Global Time Series Capitalizing over Existing Products. Part1: Principles of Development and Production. Remote Sens. Environ. 137 (October), 299–309. https://doi.org/10.1016/j.rse.2012.12.027.

Bréda, N.J.J., 2008. Leaf Area Index. In: Encyclopedia of Ecology, 1st ed. Elsevier, Oxford, Britain, pp. 2148–2154.

Darvishzadeh, R., Skidmore, A., Schlerf, M., Atzberger, C., 2008a. Inversion of a Radiative Transfer Model for Estimating Vegetation LAI and Chlorophyll in a Heterogeneous Grassland". Remote Sens. Environ. 112 (5), 2592–2604. https://doi.org/10.1016/j.rse.2007.12.003.

Darvishzadeh, R., Skidmore, A., Atzberger, C., Wieren, S.V., 2008b. Estimation of vegetation LAI from hyperspectral reflectance data: Effects of soil type and plant architecture. Int. J. Appl. Earth Obs. Geoinf. 10 (3), 358–373. https://doi.org/10.1016/j.jag.2008.02.005.

Dimitriadou, S., Nikolakopoulos, K.G., 2022. Development of the Statistical Errors Raster Toolbox with Six Automated Models for Raster Analysis in GIS Environments. Remote Sens. (Basel) 14 (21), 5446. https://doi.org/10.3390/rs14215446.

Ding, A.X., Ma, H., Liang, S.L., He, T., 2022. Extension of the Hapke Model to the Spectral Domain to Characterize Soil Physical Properties. Remote Sens. Environ. 269, 112843 https://doi.org/10.1016/j.rse.2021.112843.

Ding, Y.L., Zhang, H.Y., Zhao, K., Zheng, X.M., 2017. Investigating the accuracy of vegetation index-based models for estimating the fractional vegetation cover and the effects of varying soil backgrounds using in situ measurements and the PROSAIL model. Int. J. Remote Sens. 38 (14), 4206–4223. https://doi.org/10.1080/01431161.2017.1312617.

Ding, Y.Y., Zheng, X.M., Zhao, K., Xin, X.P., Liu, H.J., 2016. Quantifying the Impact of NDVIsoil Determination Methods and NDVIsoil Variability on the Estimation of Fractional Vegetation Cover in Northeast China. Remote Sens. 8 (1), 29. https://doi.org/10.3390/rs8010029.

Doktor, D., Lausch, A., Spengler, D., Thurner, M., 2014. Extraction of Plant Physiological Status from Hyperspectral Signatures Using Machine Learning Methods. Remote Sens. 6 (12), 12247–12274. https://doi.org/10.3390/rs61212247.

Fu, Y.Y., Yang, G.J., Wang, J.H., Feng, H.K., 2013. A Comparative Analysis of Spectral Vegetation Indices to Estimate Crop Leaf Area Index. Intell. Autom. Soft Co. 19 (3), 315–326. https://doi.org/10.1080/10798587.2013.824176.

Gao, L., Darvishzadeh, R., Somers, B., Johnson, B.A., et al., 2022. Hyperspectral response of agronomic variables to background optical variability: Results of a numerical experiment. Agric. For. Meteorol. 326, 109178 https://doi.org/10.1016/j.agrformet.2022.109178.

Garrity, D., Bindraban, P., 2004. A Globally Distributed Soil Spectral Library Visible Near Infrared Diffuse Reflectance Spectra, World Agroforestry Centre (ICRAF). Nairobi, Kenya, pp. 1–8.

Hapke, B., 1993. Theory of reflectance and emittance spectroscopy. Cambridge University Press, Cambridge England and New York, NY, USA, pp. 369–395.

Huete, A.R., 1989. Soil influences in remotely sensed vegetation canopy spectra. In: Asrar, G. (Ed.), Theory and Applications of Optical Remote Sensing. Wiley, New York.

Huete, A.R., Jackson, R.D., Post, D.F., 1985. Spectral response of a plant canopy with different soil backgrounds. Remote Sens. Environ. 17 (1), 37–53. https://doi.org/10.1016/0034-4257(85)90111-7.

Hupet, F., Lambot, S., Javaux, M., Vanclooster, M., 2002. On the identification of macroscopic root water uptake parameters from soil water content observations. Water Resour. Res. 38 (12), 1300. https://doi.org/10.1029/2002WR001556.

Jacquemoud, S., Verhoef, W., Baret, F., Bacour, C., Zarco-Tejada, P.J., Asner, G.P., François, C., Ustin, S.L., 2009. PROSPECT+SAIL Models: A Review of Use for

Vegetation Characterization. Remote Sens. Environ. 113, S56–S66. https://doi.org/10.1016/j.rse.2008.01.026.
Jia, K., Liang, S.L., Gu, X.F., Baret, F., Wei, X.Q., Wang, X.X., Yao, Y.J., Yang, L.Q., Li, Y. W., 2016. Fractional Vegetation Cover Estimation Algorithm for Chinese GF-1 Wide Field View Data. Remote Sens. Environ. 177, 184–191. https://doi.org/10.1016/j.rse.2016.02.019.
Jiang, C.Y., Fang, H.L., 2019. GSV: A General Model for Hyperspectral Soil Reflectance Simulation. Int. J. Appl. Earth Obs. Geoinf. 83, 101932 https://doi.org/10.1016/j.jag.2019.101932.
Knyazikhin, Y., Martonchik, J.V., Myneni, R.B., Diner, D.J., Running, S.W., 1998. Synergistic Algorithm for Estimating Vegetation Canopy Leaf Area Index and Fraction of Absorbed Photosynthetically Active Radiation from MODIS and MISR Data. J. Geophys. Res. 103 (D24), 32257–32275. https://doi.org/10.1029/98JD02462.
Liu, D.Y., Jia, K., Jiang, H.Y., Xia, M., Tao, G.F., Wang, B., Chen, Z.L., Yuan, B., Li, J., 2021. Fractional Vegetation Cover Estimation Algorithm for FY-3B Reflectance Data Based on Random Forest Regression Method. Remote Sens. 13 (11), 2165. https://doi.org/10.3390/rs13112165.
Marandi, M., Parida, B.R., Ghosh, S., 2022. Retrieving Vegetation Biophysical Parameters and GPP Using Satellite-Driven LUE Model in a National Park. Environ. Dev. Sustain. 24 (7), 9118–9138. https://doi.org/10.1007/s10668-021-01815-0.
Nilson, T., 1971. A Theoretical Analysis of the Frequency of Gaps in Plant Stands. Agric. Meteorol. 8, 25–38. https://doi.org/10.1016/0002-1571(71)90092-6.
Price, J.C., 1990. On the Information Content of Soil Reflectance Spectra. Remote Sens. Environ. 33 (2), 113–121. https://doi.org/10.1016/0034-4257(90)90037-M.
Prudnikova, E., Savin, I., Vindeker, G., Grubina, P., Shishkonakova, E., Sharychev, D., 2019. Influence of Soil Background on Spectral Reflectance of Winter Wheat Crop Canopy. Remote Sens. 11, 1932. https://doi.org/10.3390/rs11161932.
Qian, X.W., Liu, L.Y., 2020. Retrieving Crop Leaf Chlorophyll Content Using an Improved Look-Up-Table Approach by Combining Multiple Canopy Structures and Soil Backgrounds. Remote Sens. (Basel) 12 (13), 2139. https://doi.org/10.3390/rs12132139.
Tao, G.F., Jia, K., Wei, X.Q., Xia, M., Wang, B., Xie, X.H., Jiang, B., Yao, Y.J., Zhang, X.T., 2021. Improving the Spatiotemporal Fusion Accuracy of Fractional Vegetation Cover in Agricultural Regions by Combining Vegetation Growth Models. Int. J. Appl. Earth Obs. Geoinf. 101, 102362 https://doi.org/10.1016/j.jag.2021.102362.
Vamborg, F.S.E., Brovkin, V., Claussen, M., 2011. The Effect of a Dynamic Background Albedo Scheme on Sahel/Sahara Precipitation during the Mid-Holocene. Clim. Past 7 (1), 117–131. https://doi.org/10.5194/cp-7-117-2011.
Verrelst, J., Dethier, S., Rivera, J.P., Munoz-Mari, J., Camps-Valls, G., Moreno, J., 2016. Active Learning Methods for Efficient Hybrid Biophysical Variable Retrieval. IEEE Geosci. Remote Sens. Lett. 13 (7), 1012–1016. https://doi.org/10.1109/lgrs.2016.2560799.
Wang, B., Jia, K., Liang, S.L., Xie, X.H., Wei, X.Q., Zhao, X., Yao, Y.J., Zhang, X.T., 2018. Assessment of Sentinel-2 MSI Spectral Band Reflectances for Estimating Fractional Vegetation Cover. Remote Sens. 10 (12), 1927. https://doi.org/10.3390/rs10121927.
Weiss, M., Baret, F., Myneni, R.B., Pragnère, A., Knyazikhin, Y., 2000. Investigation of a Model Inversion Technique to Estimate Canopy Biophysical Variables from Spectral and Directional Reflectance Data. Agronomie 20 (1), 3–22. https://doi.org/10.1051/agro:2000105.
Xia, M., Jia, K., Zhao, W.W., Liu, S.L., Wei, X.Q., Wang, B., 2021. Spatio-Temporal Changes of Ecological Vulnerability across the Qinghai-Tibetan Plateau. Ecol. Ind. 123, 107274 https://doi.org/10.1016/j.ecolind.2020.107274.
Xie, Q.Y., Dash, J., Huete, A., Jiang, A.H., Yin, G.F., Ding, Y.L., Peng, D.L., Hall, C.C., Brown, L., Shi, Y., Ye, H.C., Dong, Y.Y., Huang, W.J., 2019. Retrieval of Crop Biophysical Parameters from Sentinel-2 Remote Sensing Imagery. Int. J. Appl. Earth Obs. Geoinf. 80, 187–195. https://doi.org/10.1016/j.jag.2019.04.019.
Younes, N., Joyce, K.E., Northfield, T.D., Maier, S.W., 2019. The Effects of Water Depth on Estimating Fractional Vegetation Cover in Mangrove Forests. Int. J. Appl. Earth Obs. Geoinf. 83, 101924 https://doi.org/10.1016/j.jag.2019.101924.
Zhang, Z.C., Li, W.J., Xin, Q.C., 2020. Machine learning-based modeling of vegetation leaf area index and gross primary productivity across North America and comparison with a process-based model. J. Adv. Model Earth Syst. 13, e2021MS002802. 10.1029/2021MS002802.